Meteoritics & Planetary Science 41, Nr 5, 797–813 (2006)
Abstract available online at http://meteoritics.org

Alkali-feldspathic material entrained in Fe,S-rich veins in a monomict ureilite

Paul H. WARREN*, Heinz HUBER, and Finn ULFF-MØLLER

Institute of Geophysics, University of California—Los Angeles, Los Angeles, California 90095–1567, USA
*Corresponding author. E-mail: pwarren@ucla.edu

(Received 21 July 2005; revision accepted 04 January 2006)

Abstract–The Elephant Moraine (EET) 96001 ureilite contains a remarkable diversity of feldspars, which occur as tiny (no more than 60 μm maximum dimension) grains within a few Fe,S-rich (now weathered to mostly Fe oxide) veins. Molar S:Fe ratio in the veins averages 0.08 ± 0.02. The veins meander and feature large fluctuations in apparent width; they appear to have entered this monomict breccia by a gentle, percolative process, not by violent impact injection. The feldspars are accompanied by a diverse suite of K-rich (and generally also Ti-rich) feldspathic glasses, and also major proportions of silica and pyroxene, which is largely fassaitic. A rhönite-like phase is also found, and, as inclusions in one of the fassaites, a Cr-poor spinel-like phase. The feldspars mostly feature remarkably high K/Na compared to feldspars of comparable An from polymict ureilites. The EET 96001 feldspathic component was probably once part of a thin basaltic crust on a ureilite asteroid. The spinel included in one of the fassaites formed at remarkably high fO_2 (apparent oxidation state of iron: ~41 atom% Fe^{3+}), suggesting that the parent magma possibly assimilated near-surface water (however, the Fe^{3+} was not directly measured, and has conceivably been affected by terrestrial weathering; also, there is no assurance that this fassaite originated together with the typical feldspar). We speculate that the feldspathic component was mixed into the dense, Fe,S-rich vein material, and very soon thereafter the Fe,S-rich vein material was emplaced adjacent to the EET 96001 host ureilite, at an advanced stage in a chaotic catastrophic disruption and partial reassembly process that affected all ureilites. The high-K nature of the EET 96001 feldspathic component, including the feldspathic glasses, suggests that fractional fusion may not have been as common during ureilite anatexis as has been inferred from recent studies of clast assemblages in polymict ureilites.

INTRODUCTION

Ureilites are a common and distinctive type of achondrite. As reviewed by Goodrich et al. (2004), their number has reached over one hundred, which qualifies them, after HED meteorites, as one of the two most numerous types of achondrite. Ureilites are essentially extremely depleted peridotites, presumably from the mantle(s) of one or more asteroids. As reviewed by Mittlefehldt et al. (1998) and Warren et al. (2006), they show considerable diversity in terms of proportions of olivine, pigeonite, orthopyroxene, and augite, and yet they are remarkably consistent in several other respects. They virtually always contain important proportions (average 3 wt%) of carbon, mostly as either amorphous "C matrix" or, in some of the lowest-shock ureilites, graphite. The rims of their olivines show distinctive indications of FeO reduction: tiny inclusions of Fe metal scattered amid olivine that is reverse-zoned toward pure Mg olivine (and typically also, just beyond the rims, either Mg pyroxene or silica). The complementary oxidation presumably converted some fraction of former solid carbon into CO gas. In contrast, the mafic-silicate cores in any individual monomict ureilite are remarkably uniform in composition. Ureilites invariably exhibit a remarkably step-wise cooling history: slow at first, but very rapid later (Miyamoto et al. 1985; Takeda et al. 1989). Most important in connection with this study is that monomict ureilites are virtually devoid of feldspar. Until now, only vague mention has ever been made of feldspar within a monomict ureilite. An_{22} (Bland 1993) and An_{36} grains (Mason 1998) were mentioned in Frontier Mountain (FRO) 90168 and Elephant Moraine (EET) 96001, respectively.

Even polymict ureilites, some of which contain solar-wind-derived noble gases, which implies surface-regolith derivation (Ott et al. 1993; Rai et al. 2003), contain only tiny proportions of feldspar. Bulk analyses of five polymict ureilites (Warren et al. 2006) contain, on average, 0.54 ± 0.06 wt% Al_2O_3. Since ~30 wt% (at least 20 wt%) of these polymict ureilites consists of pyroxene with, on average,

~1 wt% (at least 0.8 wt%) Al_2O_3 (Mittlefehldt et al. 1998), and even highly alkalic feldspar, say $An_{10}Ab_{80}Or_{10}$, contains at least 21 wt% Al_2O_3, by mass balance an average polymict ureilite contains roughly 1 wt% (at most 1.8 wt%) feldspar. To account for the dearth of feldspar (i.e., basalt) among meteorites of possible ureilitic affinity, the most widely discussed model postulates that the ureilite-associated basalts tended to be blown clear off the parent asteroid by an extraordinarily explosive style of volcanism that occurs when CO-rich magmas erupt at the surface of small atmosphereless bodies (Warren and Kallemeyn 1992; Scott et al. 1993; Goodrich et al. 2004; originally suggested for aubrite-related basalts by Wilson and Keil 1991).

EET 96001 is a small (5.79 g) ureilite that is brecciated (an uncommon phenomenon among ureilites) and possibly as a whole-rock polymict. Goodrich et al. (2004) classified it as polymict, but also indicated this was not based on anything "beyond initial description" (i.e., Mason 1998). Mason (1998) did not specifically address whether it is polymict or monomict. He described the rock as a "microbreccia," mentioned "one grain" of plagioclase, and cited a wide range of olivine compositions, $Fo_{75–84}$. However, variable olivine composition is a hallmark of all ureilites, unless the reduced rims are excluded from the database (Mason did not specify whether his olivine compositional range differentiated between cores and rims).

Mason (1998) said nothing about the size of the plagioclase grain he analyzed in EET 96001. The overwhelming majority of all silicate grains in EET 96001 are several hundreds of μm (up to 1.2 mm) across. When we initially inspected our allocation, thin section EET 96001,7, it appeared that we had unfortunately missed the feldspar component; which would not be surprising considering that Mason (1998) reported merely "one grain" in thin section EET 96001,3, and considering the paucity of feldspar among ureilites in general. However, many months later, we scrutinized EET 96001,7 very carefully and noted the presence of numerous tiny grains of not only feldspar but also associated basaltic-silicic materials. In this paper, we report on the mineralogy and textural context of these feldspathic components and discuss implications for ureilite petrogenesis.

METHODS

Mineral compositions were determined using wavelength-dispersive detectors on UCLA's JEOL JXA-8200 electron probe. In general, analyses were run at an accelerating voltage of 15 keV, with focused beam and count durations of 15–20 s. However, for volatilization prone phases (alkali feldspars and glasses), currents as low as 3 nA, beam diameters as wide as 3 μm, and ~0.5× shorter count times were employed. Semiquantitative analyses of the groundmasses of Fe,S veins and a few silicate grains too tiny for quantitative analysis were obtained using an EDAX system on a LEO 1430 SEM. In addition, bulk compositional data for a 316 mg chip of EET 96001 were obtained by INAA; the technique and complete data set are reported in Warren et al. (2006).

DESCRIPTION OF THE HOST ROCK AND FELDSPATHIC VEINS

Thin section EET 96001,7 shows a lightly brecciated but apparently monomict ureilite (Fig. 1). The sole primary mafic silicates (i.e., excluding components of the feldspathic veins and products of the late-stage "smelting" redox process) are olivine and pigeonite. The shock stage is moderate (s2); mosaicism is rare or absent in the olivine (Rubin 2006). The cores of the olivines and pigeonites are as uniform in composition as in any monomict ureilite (Table 1; Figs. 2 and 3). Mason (1998) reported a wide range in olivine mg (= mol% MgO/[MgO + FeO]), 75–84, and an average of 80 (number of analyses unstated), but we found no stoichiometric olivine more ferroan that mg = 80.6. As usual among monomict ureilites, pigeonite cores are remarkably uniform in composition; it is an analytical challenge to resolve any significant major-element variation.

Two or three distinct feldspathic veins were eventually found in EET 96001,7. Figure 1 shows the broad context of the largest vein system. The small, isolated vein that we designate vein 2 (Fig. 4) is separated by ~8 mm from the principal vein, which we designate 1A (Figs. 1, 5, and 6). But the vein that we designate 1B (Fig. 6) is close to one end of vein 1A, at a place where both 1A and 1B are truncated by the edge of the thin section. Assuming both 1A and 1B originally extended just ~100 μm further into the off-section space, they were probably once connected. Arguably, their inward extensions already connect at a point shortly below the lower left corner of Fig. 5.

We use the term feldspathic veins in a relative sense. The veins consist mainly of iron oxide. This vein groundmass matter, which probably represents a mixture of ultrafine-grained phases, is presumably a weathering product. The vein groundmass consistently contains, at resolvable scales, roughly 2 wt% chlorine and several wt% sulfur. Semiquantitative EDS-based analyses (27) indicate that the molar S:Fe ratio averages 0.08 ± 0.02. The nature of the original groundmass is unclear. The Cl component (likely) and the S component (conceivably) are results of weathering. However, for an Antarctic (weathering class B) meteorite, such a gross and uniform addition of S seems unlikely. Moreover, the veins apparently oozed through the rock (see below), and for pure FeNi without an S component, the temperature required for complete melting would be implausibly high. Thus, we infer the S is at least mostly preterrestrial. At sufficiently low brightness settings in backscattered electron imagery (e.g., Fig. 6) the vein groundmass shows a structure of fine-scale concentric banding, with the bands commonly undulate, but tending to

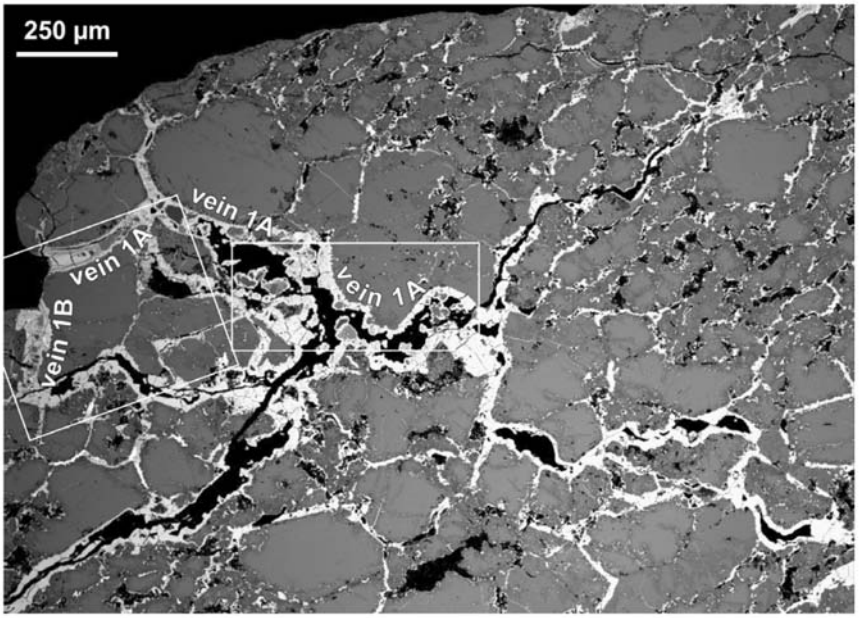

Fig. 1. A backscattered electron image of EET 96001,7 showing the main 1A feldspathic vein and also the nearby vein 1B. The boxes show the regions of Figs. 5 and 6.

parallel the vein walls in a pattern that suggests the crystallization generally started along the vein walls and progressed in toward the vein centers. The banding is conceivably entirely the result of terrestrial weathering, but structural relationships involving banding, cracks, and obvious weathering products within cracks, suggest that the present banding is more likely the weathered equivalent of a similar structure within the preterrestrial veins. Lining the walls of vein 1B are layers of magnetite that are probably weathered derivatives of Ni-poor kamacite (Fig. 6), consistent with in situ fractional crystallization of a moderately S-rich (i.e., S:Fe of order 0.1) metallic melt.

Most of the feldspathic matter occurs as tiny, single-phase grains, often with rounded shapes suggesting corrosive or erosive loss of mass. In four instances, multiple phases large enough for separate analysis are in contact: three instances of glass containing crystalline silicate microphenocrysts, and one instance of spinel(?) inclusions within fassaitic pyroxene. As a means of flagging these associations, we employ designations for their individual constituent phases that end with a one-letter designation for the association: A for an enclave of glass containing alkali feldspar, M for an enclave with a glassy mesostasis-like texture, P for an enclave of glass containing plagioclase, and W for a wedge-shaped grain of fassaite with spinel(?) inclusions. Otherwise, our nomenclature scheme for the analyzed grains (Table 1) is simply numerical.

The Veins Were Probably Not Violently Injected

The detailed textures of the feldspathic veins indicate that their emplacement into the volume of EET 96001 was a slow and gentle process, not an instantaneous and violent impact-injection. The feldspathic veins meandered between large mafic silicate host grains instead of smashing through them. Consider the main 1A vein, starting from its "origin" near the "northwest" corner of Fig. 1. The vein first extends "northeast" for ~330 µm between the concave edge of an olivine (north of the vein) and the convex edge of a pigeonite (south of the vein). At the 330 µm point, continuation in the same direction would have caused the vein to split a large roundish olivine in half. Instead, the vein takes an ~80° right turn. (At this point an apparent subvein, albeit lacking in feldspathic components, extends north, neatly between two unbroken olivine crystals.) After an east-southeast trending length of ~140 µm between the large olivine and a diamond-shaped grain or fragment of extensively reduced olivine, the vein opens out into a far wider domain, roughly 200–300 µm across, that continues for ~500 µm in a roughly southeast direction until, at fassaite 1W, it bifurcates into two thinner subveins; one subvein, which we regard as the main 1A vein, continues to the southeast, the other subvein extends for at least a short distance to the southwest (however this southwesterly subvein has no feldspathic components, and after only ~150 µm southwest of fas 1W becomes difficult to distinguish from an ordinary crack). At ~100 µm southeast of fas 1W, the main 1A vein takes an abrupt 90° turn to the left, in conformity with a pre-existing angular boundary between the open-jaw-shaped edge of a large pigeonite ("north" of the vein; the "jaws" open to the "south") and a partially disrupted olivine; this northeastward length of the vein extends for ~150 µm. Then, at the approximate position of feldspar 2A, still in conformity with the edge of the open-jaw-shaped pigeonite, the vein turns again, ~90° to the right, and also

Table 1. Phase compositions in EET 96001,7 determined by EPMA (oxides are in wt%; ratios in mol%).

Phase	Designation	Description	N^a	SiO_2	MgO	Na_2O	Al_2O_3	FeO	MnO	Cr_2O_3	K_2O	CaO	TiO_2	V_2O_3	Sum	An	Ab	Or	Stoichiometry[b]	
Plagioclase	f 1P	40 × 15 μm rect. grain in glass 1P	8	51.16	0.11	3.84	29.79	1.46	0.02	0.03	0.33	12.83	0.18		99.75	63.6	34.5	1.9	5.02	0.999
Alkali-feldspar	f 2A	15 × 7 μm grain in glass 5A	4	66.06	0.01	7.50	17.94	2.16	0.04	0.10	5.63	0.55	0.11		100.10	2.6	65.2	32.2	5.03	1.004
Alkali-feldspar	f 3	60 × 15 μm subhedral grain	7	65.29	0.01	7.24	19.16	1.37	0.01	0.03	5.70	0.91	0.07		99.77	4.4	63.0	32.6	5.02	1.008
Plagioclase	f 4	15 × 10 μm grain	3	55.95	0.03	5.72	26.83	1.42	0.02	0.08	0.50	9.85	0.04		100.44	47.4	49.8	2.9	5.02	1.006
Plagioclase	f 5	10 × 7 μm grain	1	64.06	0.01	9.86	22.15	1.01	0.00	0.00	0.13	2.85	0.05		100.12	13.7	85.6	0.7	5.01	0.998
Feldspar	f 6	10 × 10 μm grain	2	61.08	0.02	7.26	22.79	1.41	0.00	0.17	2.30	4.52	0.06		99.63	22.2	64.4	13.4	5.02	0.994
Na-feldspar	f 7	15 × 5 μm grain	1	66.77	0.04	10.96	19.22	1.50	0.00	0.00	0.36	0.27	0.04		99.16	1.3	96.6	2.1	5.01	0.984
K-feldspar	f 8	20 × 10 μm grain	4	64.22	0.01	1.07	18.61	1.22	0.01	0.04	15.75	0.02	0.11		101.05	0.1	9.4	90.5	5.04	1.036
																				mg
Glass	g 1P	Host for feldspar 1P	2	44.09	5.45	1.63	14.37	14.83	0.22	0.04	1.66	11.28	5.34		98.90					39.6
Glass	g 2	25 × 12 μm irreg. shaped grain	5	43.53	4.46	5.03	15.73	13.27	0.22	0.04	2.31	10.33	4.41		99.36					37.5
Glass	g 3M	Host of rhönite-like phase + fas 1M	4	46.55	2.30	6.57	18.65	8.75	0.25	0.01	4.03	7.78	2.41		97.29					31.9
"Glass"	"g" 4	15 × 4 μm grain of mesostasis	3	54.18	1.15	8.07	18.97	7.84	0.27	0.06	5.92	1.59	1.28		99.33					20.7
Glass	g 5A	Host for feldspar 2A	2	63.79	0.01	5.33	11.53	10.14	0.29	0.06	4.92	1.23	0.58		97.89					0.1
Silica	s	Average, largest in-vein grains	5	98.44	0.01	0.01	0.04	0.84	0.03	0.04	0.02	0.01	0.03		99.45					
Spinel?	sp W	Tiny inclusion in fassaite 1W	6	0.19	8.53	0.00	7.49	35.0	0.51	0.02	0.01	0.53	19.19	0.86	98.82	also ~26.5 wt% Fe_2O_3				20.5
Rhönite-like phase	–	Hosted by glass 3M	3	24.00	13.20	0.97	16.98	21.75	0.19	0.00	0.05	11.96	11.49	0.65	101.25					52.0
																En	Fs	Wo		
Fassaite	fas 1W	Host for spinel? spW	5	40.94	10.70	0.57	11.42	7.55	0.10	0.10	0.01	22.71	5.64	0.29	100.03	34.2	13.5	52.2		71.6
Fassaite	fas 2M	Hosted by glass 3M	5	41.57	10.74	0.68	10.93	8.18	0.12	0.05	0.17	22.10	5.51	0.34	100.39	34.4	14.7	50.9		70.1
Pigeonite cores	–	Adjacent to felds-pathic vein	43	54.54	27.25	0.07	0.95	10.20	0.42	1.00	0.01	5.21	0.12	0.03	99.79	74.2	15.6	10.2		82.6
Pigeonite cores	–	Far from feldspathic veins	8	55.01	26.98	0.06	0.90	10.21	0.44	1.01	0.01	5.23	0.11		99.96	74.0	15.7	10.3		82.5
Ferroan pyroxene	–	20 × 12 μm, within vein	1	54.24	25.42	0.00	1.22	12.45	0.32	0.18	0.00	6.94	0.21		100.97	68.0	18.7	13.3		78.4
Ferroan pyroxene	–	20 × 12 μm (identical grain)	1	53.04	20.73	0.07	1.42	11.07	0.26	0.00	0.02	13.41	0.23		100.24	56.7	17.0	26.3		77.0
Olivine cores	–	Adjacent to feldspathic vein	82	38.96	42.92	0.01	0.04	17.34	0.41	0.58	0.00	0.37	0.04	0.01	100.69					81.5
Olivine cores	–	Far from feldspathic veins	67	39.30	42.93	0.01	0.04	17.34	0.41	0.59	0.00	0.37	0.02	0.01	101.02					81.5

[a]Number of analyses averaged (however, N for V_2O_3 is typically only about half of the overall N).

[b]For feldspars, two stoichiometry checks are shown: The ratio of summed cations per 8 oxygens, and the ratio (3Na + 3K + 2Ca)/Si. In stoichiometric feldspar, these ratios should be 5 and 1, respectively.

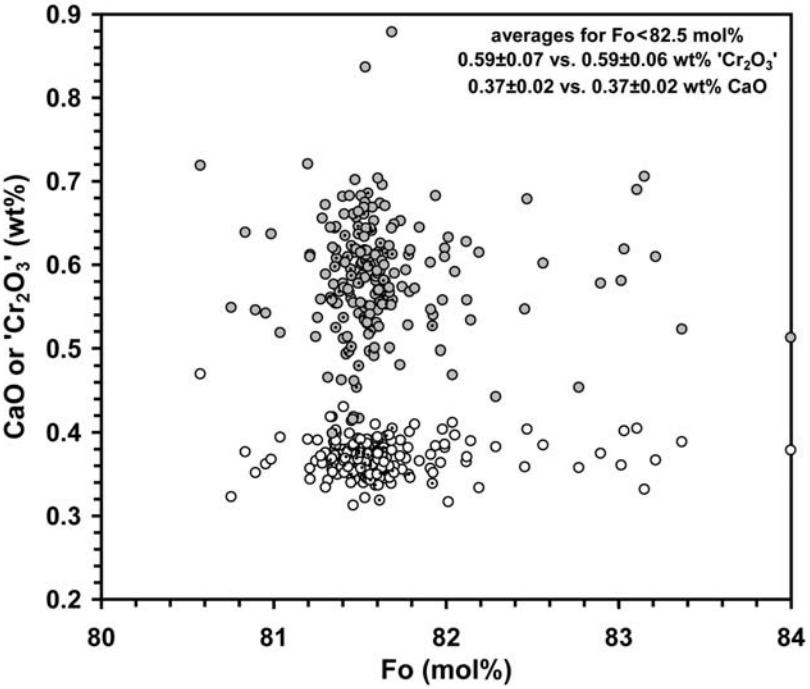

Fig. 2. Olivine-core compositions in EET 96001,7. Open symbols represent mg versus CaO; gray symbols represent mg versus "Cr_2O_3" (in quotes because much of the Cr in ureilites is probably Cr^{2+}). Symbols with small black dots at center represent grains adjacent to the 1A and 1B feldspathic veins; others represent grains well away from the 1A and 1B veins. The two populations appear identical.

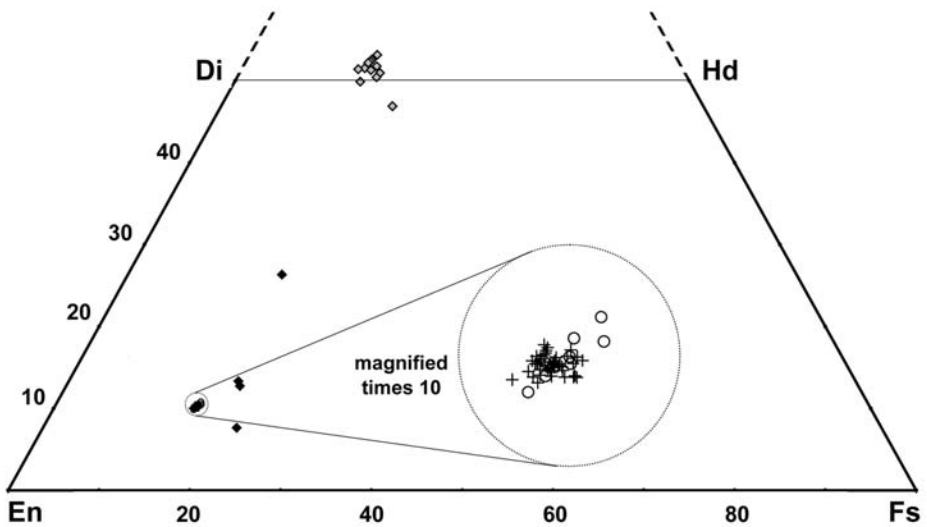

Fig. 3. Pyroxene-core Mg-Fe-Ca proportions in EET 96001,7. Crosses represent pigeonite grains adjacent to the 1A and 1B feldspathic veins; open circles represent pigeonites well away from the 1A and 1B veins. The two populations appear identical. Also shown are pyroxenes of the feldspathic component: fassaites as gray diamonds; ferroan low-Ti pyroxene as black diamonds.

widens out somewhat. No feldspathic components are found much beyond feldspar 2A, but after extending a further ~200 μm southeast, the vein appears to bifurcate and then extend considerable distances (>500 μm) in two opposite ("north" and "south") directions.

In sum, the "feldspathic" vein 1A takes at least three abrupt, near-90° turns as it meanders within 1.1 mm of the "west" end of Fig. 1. This texture suggests that the vein gently dilated the interstitial spaces between large mafic silicate host grains, which for the most part retain shapes that "fit" together. As noted by Greshake and Stöffler (2000), it is more "typical" for shock melt veins to "cut pre-existing minerals." For specific examples, see Buchanan et al. (2005), Rubin et al. (1981), Stöffler et al. (1991, especially Fig. 13), and

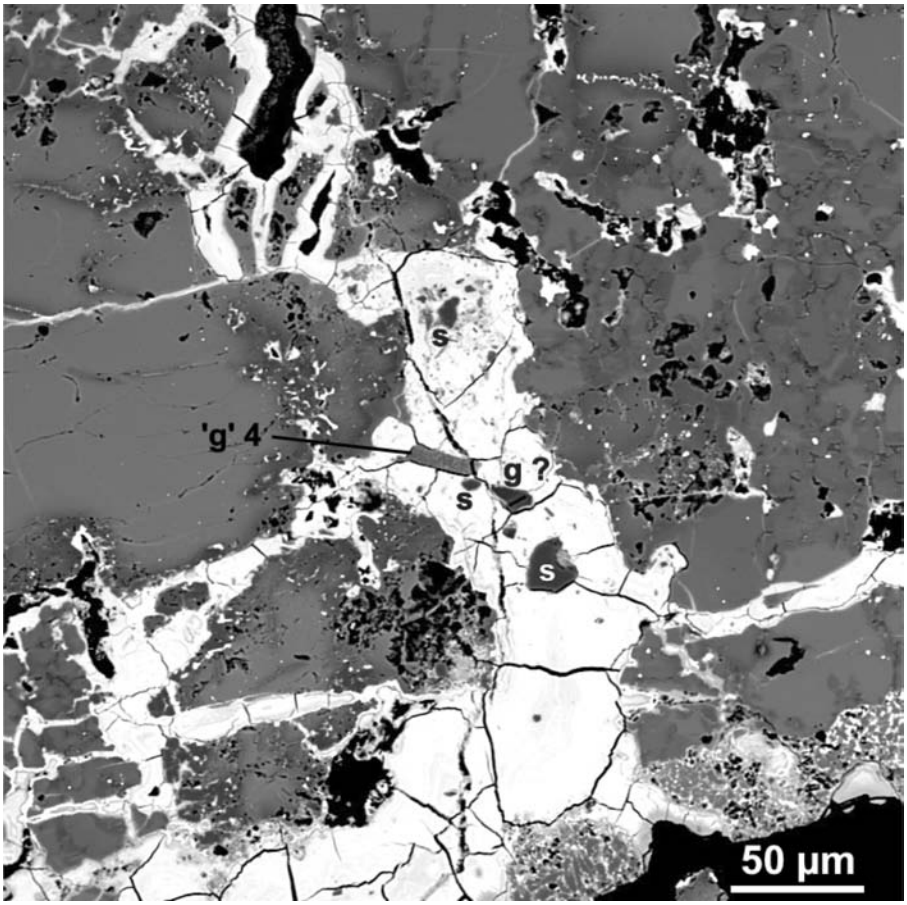

Fig. 4. A backscattered electron image of EET 96001,7 showing feldspathic vein 2, which is separated from the main 1A vein by ~8 mm. The "feldspathic" vein consists mainly of Fe oxide (white). Grey phases, except as noted, are mainly olivine and pigeonite. Abbreviations: s = silica; g = glass.

Warren and Kallemeyn (1995); however, for one counter-example, see Roedder and Weiblen (1977). The vein is far from uniform in thickness. In the area of glass 3M its width is well defined to be ~50 µm. In the general area of glass 1P the vein's width bloats out to at least 200 µm. Yet it constricts again to ~60 µm in the vicinity of fas 1W. Such grossly uneven thickness seems an unlikely attribute for a vein violently injected through a rock.

The meandering course and uneven width of the 1A vein is all the more remarkable considering that the rock appears to have been brecciated prior to the ingress of the vein matter. The reduced olivines in the lower left and upper left corners of Fig. 4 appear to have been cracked before the veining episode. So does a large mafic silicate (pigeonite) that occupies most of the "southeast" quadrant of Fig. 6 and also extends into the lower left corner of Fig. 5 (cf. Fig. 1 for overview). Significantly, in several places where the veins bifurcate to pass on both sides of loose host-rock debris (the fragmented pigeonite that straddles Figs. 5 and 6 is an especially large example), the loose host-rock mineral fragment appears nearly intact, not shattered, and displaced by no more than a small fraction of a millimeter. Such modest displacements are another indication that the Fe,S matter was probably emplaced in a slow and gentle way.

A further manifestation of gentle emplacement of the vein matter is the situation of the glass 3M enclave (Figs. 6–7). This enclave is stuffed lengthwise into the vein, at a location where the vein is not much wider than the short dimension of the fatter "west" end of the enclave. Even a slight change in the orientation of this enclave would have caused it to break, if forced, against the walls of the vein. Of course, we are only viewing a two-dimensional slice through the rock. Still, the enclave's orientation appears to have developed in response to its local surroundings, which seems an unlikely outcome unless the process of emplacement was comparatively slow and gentle.

Mafic-silicate compositions in the vicinity of the feldspathic veins show no indication for the veins being associated with any exotic ureilitic (i.e., coarse olivine and pyroxene) matter; i.e., the feldspathic veins pass between materials entirely normal for the EET 96001 ureilite. Average mafic-silicate core compositions are shown in Table 1, and the mg, CaO and "Cr_2O_3" contents of the olivines are plotted in Fig. 2. Despite great scatter (probably mostly real

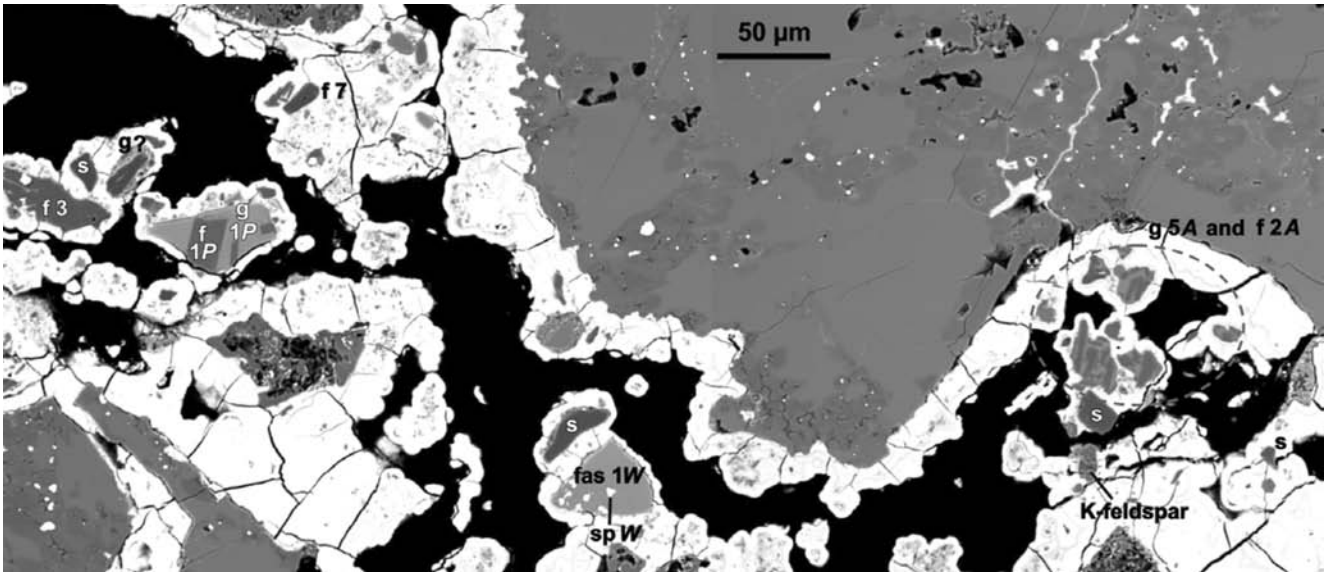

Fig. 5. A backscattered electron image of EET 96001,7 showing about half of the length of the main 1A feldspathic vein. Analyzed feldspathic-component grains are annotated as explained in the text. Abbreviations: f = feldspar; fas = fassaite, g = glass, s = silica, sp = spinel.

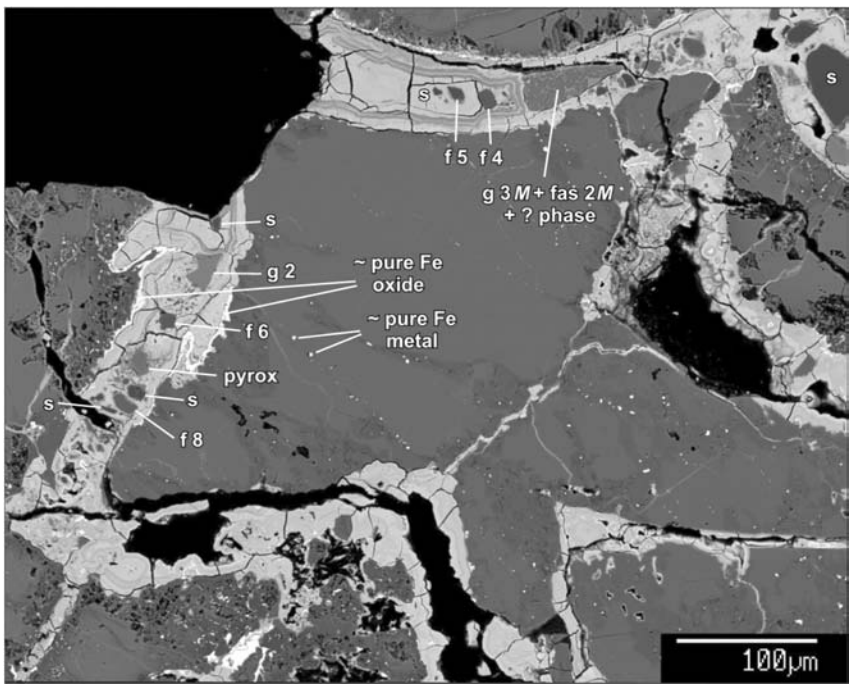

Fig. 6. A backscattered electron image of EET 96001,7 showing the 1B feldspathic vein and a portion of the main 1A feldspathic vein. Analyzed feldspathic-component grains are annotated as explained in the text. Abbreviations are as in Fig. 5.

heterogeneity) in the CaO and "Cr_2O_3" data, the compositions of the olivines adjacent to the veins are impressively similar to the compositions of olivines from widely scattered locations elsewhere in EET 96001,7. The compositional match between vein-adjacent and vein-distant pigeonite is even more impressive. Major-element proportions are shown in Fig. 3, and note (Table 1) that the minor elements Cr, Mn, Ti, and Na also show precise matches.

Mineralogy of the Feldspathic Component

Using estimates for the dimensions of the individual grains that collectively comprise the EET 96001 vein-feldspathic component, we estimated a mode for the feldspathic component, i.e., all of the manifestly exotic ingredients of the Fe,S-rich veins, apart from the Fe,S oxides and kamacite. This mode has roughly (in vol%): 24% glass,

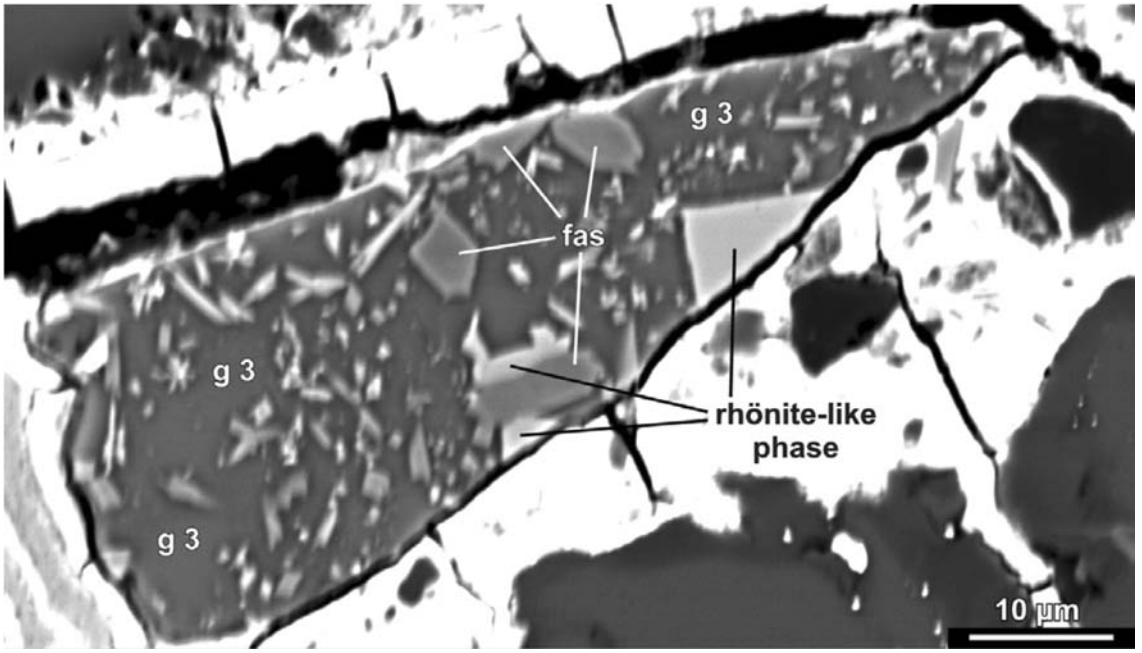

Fig. 7. A backscattered electron image of EET 96001,7 showing the glassy "M" enclave in vein 1A.

found as ~7–8 separate grains (including several that have partially devitrifed); 33% silica as ~10 separate grains up to 60 µm across; 18% alkali feldspar as ~10 separate grains up to 60 × 15 µm; 17% pyroxene, as two fassaitic grains and one 1 low-Ti ferroan grain; 7% plagioclase as ~4 separate grains up to 40 × 15 µm; 1% of a rhönite-like phase, confined to a single enclave (Fig. 7; Table 1); and a trace of spinel(?) found as tiny inclusions in fassaite 1W (Fig. 5). The numbers of separate grains are approximate because many of the smallest grains are not amenable to quantitative analysis. The feldspars are crystalline, not maskelynite.

The silica grains are consistently Al-poor ($Al_2O_3 < 0.11$ wt%) and most likely quartz. Conceivably some are olivine-FeO-to-Fe "smelting" products. However, silica occurs together with K-rich feldspathic glass (as well as plagioclase, pyroxene, ilmenite, and phosphates) in igneous clast "B1" of the Dar al Gani (DaG) 319 polymict ureilite (Cohen et al. 2004). The "feldspathic" pyroxenes obviously formed apart from the host EET 96001 ureilite, because mg is much lower (Fig. 3) in the ferroan low-Ti pyroxene, and in both the ferroan low-Ti and the fassaitic pyroxenes minor element ratios such as Fe/Mn and especially Fe/Cr are vastly higher than normal for ureilite pyroxene (Fig. 8).

The feldspars of EET 96001 have, with two (physically) small exceptions, distinctively high K/Na ratio in comparison to the feldspars found in polymict ureilites (Fig. 9). One of the exceptions, albitic feldspar f 5, occurs in intimate association with a typically K-rich plagioclase, f 4 (Fig. 6); apparently, these two compositionally disparate feldspars were introduced into the "west" end of vein 1A simultaneously.

The tiny opaque inclusions in fas 1W (Fig. 5) are, if truly spinels, remarkably Fe_2O_3-rich. Analyses yield good sums only if roughly one-half of the Fe is assumed to be ferric, and spinel stoichiometry (three cations per four oxygens) only if ~41 atom% of the total Fe is assumed ferric (Table 1); i.e., the inclusions appear to be Mg-bearing titanomagnetites. Conceivably they, or more precisely the one inclusion large enough for quantitative analysis, underwent oxidation during Antarctic weathering. However, the survival of good pyroxene stoichiometry for the host fas 1W suggests that weathering was probably not intense enough to heavily alter an inclusion so deep (at least, according to the two-dimensional thin section) within fas 1W.

The rhönite-like phase is far more FeO-rich than the rhönites reported from high-temperature inclusions in the Allende and Efromovka CV3 chondrites (e.g., Nazarov et al. 2000). The EET 96001 phase probably formed at a less extremely low fO_2 than that (~10^{-18} atm) inferred for the CV3 phase (Beckett et al. 1986). However, a single 5 µm grain of CaS (oldhamite) included in a corroded olivine rim adjacent to vein 1A, and only ~27 µm from the *M* enclave rhönite, also might reflect uncommonly low fO_2.

All five analyzed glasses (Table 1) are at the scales analyzed (typically 3 µm) internally homogeneous, such that real variations are difficult to distinguish from analytical scatter. Nonetheless, these glasses are remarkably diverse. We note apparent correlations between MgO (or mg) and other major oxides (Fig. 10), but limited statistics imply these correlations are not necessarily significant. The magnesian glasses g 1P and g 2 have 4.4–5.3 wt% TiO_2. The two glasses that have low MgO and moderate TiO_2 have 4.9–5.9 wt% K_2O. Several otherwise grossly dissimilar glasses, g 1P and

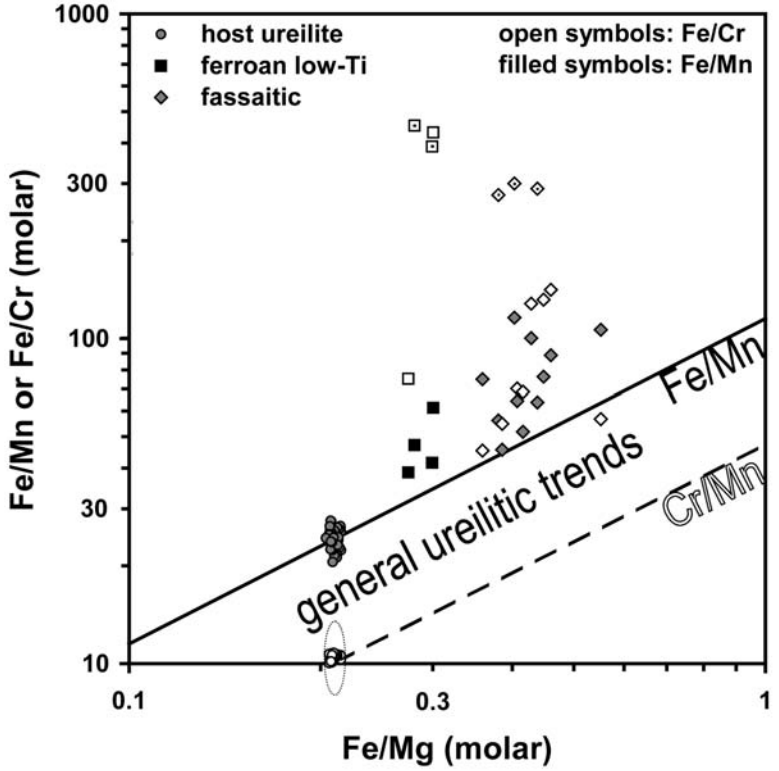

Fig. 8. Fe/Mg versus Fe/Mn and Fe/Cr for pyroxenes in EET 96001,7. The host ureilite's pigeonites (core compositions) plot squarely on the overall trends for ureilites (Mittlefehldt et al. 1998). The exotic pyroxenes found in the feldspathic veins have Fe/Mn and especially Fe/Cr well off the ureilite trends. For five of the Fe/Cr values, indicated by black dots within otherwise unfilled symbols, the plotted results are actually Fe/Cr lower limits. For plotting convenience, only a subset of the individual host-ureilite Fe/Cr results are shown; dotted oval indicates actual range.

g 5, both have remarkably high K/Na ratio. The glass in clast B1 in the DaG 319 polymict ureilite (Cohen et al. 2004) compositionally resembles the most MgO-poor (g 5*A*) EET 96001 glass, but the DaG 319 glass is more SiO_2-rich (69–72 wt%) and generally poorer in other major elements (e.g., Al_2O_3 ~ 9 wt%).

DISCUSSION

Bulk Composition of EET 96001

Warren et al. (2006) report a bulk analysis of this ureilite. The feldspar-associated elements Al, Na, and K are at ordinary ureilite levels (Fig. 11); if anything K, for which only an upper limit could be determined, is uncommonly low. Incompatible trace elements such as Sm also show nondescript concentrations. These data confirm indications from thin section EET 96001,7: The total feldspathic component is only a tiny trace of the bulk rock.

Of possibly greater significance are the siderophile-element results found by Warren et al. (2006). The "noble" siderophile elements Ir and Os are unusually high, especially considering that EET 96001 has a moderate olivine-core mg, because the highest Ir and Os concentrations tend to occur among very low-mg ureilites. Elements such as Ni and As that are highly siderophile, but not so "nobly" siderophile as Ir and Os, are extraordinarily high in EET 96001 (Fig. 12). In general, such elements are far more depleted than Ir in ureilites, and Warren et al. (2006) propose that the depletion mechanism involved down-percolation of S-rich metallic melts comparable to the inferred original, pre-weathering, veins of EET 96001, i.e., Fe,S-rich veins of the same general type as the "feldspathic" veins. The high Ni and As (etc.) of EET 96001 may reflect an unusually high abundance of Fe,S-vein matter within this meteorite. Sample representativeness is conceivably a problem, but for As, Ni, and other siderophile elements, Warren and Kallemeyn (1992) and Warren et al. (2006) found excellent agreement (in comparison to the factor of 10 ranges manifested in Fig. 12) between separate chips of mass very similar to, often smaller than, the 316 mg analyzed from EET 96001.

Possible Relationship with Polymict Ureilites

EET 96001 is a breccia, and its proximity to the EET 83309 and EET 87720 polymict ureilites in Fig. 12 raises the possibility that despite the mineralogical uniformity we found in EET 96001,7 (apart from the distinctive Fe,S-feldspathic

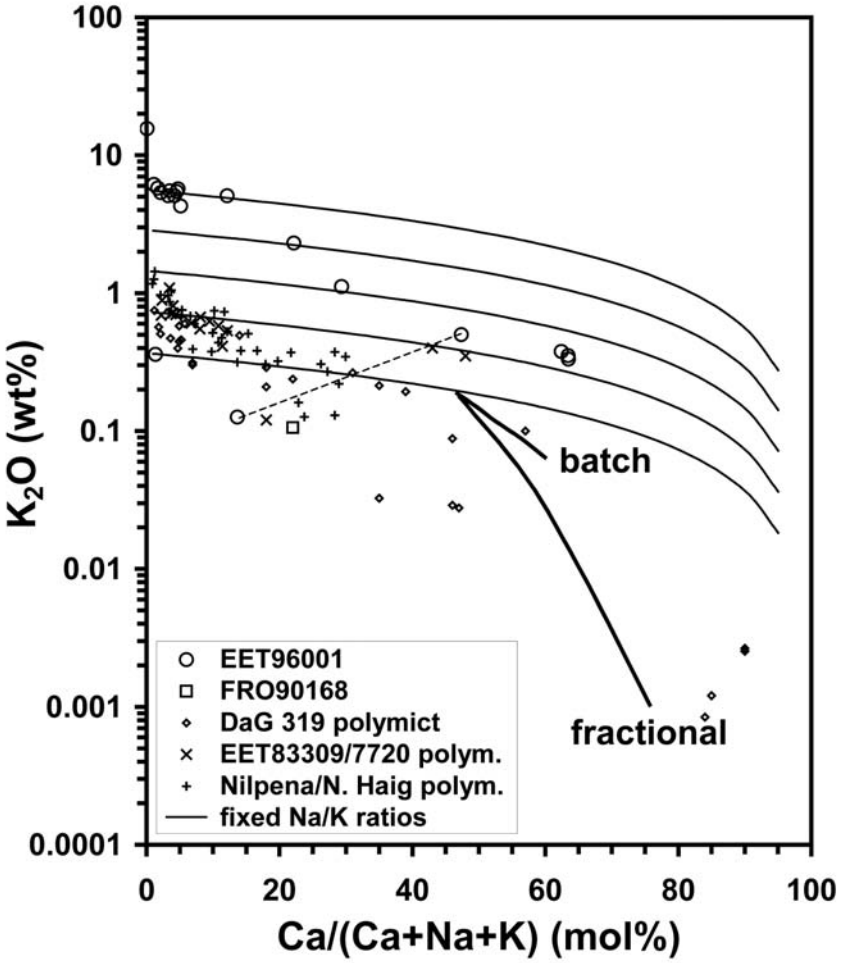

Fig. 9. Plagioclase compositions in EET 96001 and, for comparison, FRO 90168 (Bland 1993) and several polymict ureilites, using a plot format originated by Kita et al. (2004). The vast majority of EET 96001 feldspars have distinctly K-rich compositions in comparison to the polymict-ureilitic feldspars. Tie line (dashed) denotes a pair of feldspars that occur in close proximity within vein 1A (Fig. 6) and yet show grossly different affinities on this plot. Polymict ureilite data are from Prinz et al. (1987), Kita et al. (2004), Cohen et al. (2004), Guan and Crozaz (2001), and Warren and Kallemeyn (1992). The fixed Na/K ratios plotted are weight ratios of 10, 20, 40, 80, and 160. Note that the groupings of EET 83309 with EET 87720 and of Nilpena with North Haig are done only for the sake of minimizing complexity in this diagram; they are not meant to imply pairings. Also shown are plagioclase compositions predicted to form by "MELTS" models of Kita et al. (2004), with an assumed CM chondrite starting material, and assumed genesis of the parent magma by either equilibrium (batch) or fractional (Rayleigh) partial melting. These models are discussed in the text.

veins, which clearly entered the rock by gentle oozing rather than by violent impact-injection), it might be a piece of the same polymict ureilite(s) as EET 83309 or EET 87720. Weighing against this model, however, is the obvious difference between the preponderant feldspar compositional type in EET 96001 versus the typical feldspars of EET 83309, EET 87720, and for that matter all known polymict ureilites (Fig. 9).

The fassaitic pyroxenes in EET 96001 are also distinctive. Prinz et al. (1987) studied pyroxenes associated with the feldspathic components of polymict ureilite EET 83309. Based on their Mg-Fe-Ca quadritateral diagram and, tacitly, their brief text, they found no EET 83309 pyroxenes comparable to the fassaitic pyroxenes of EET 96001. The polymict ureilites DaG 319 (Ikeda et al. 2000), Nilpena (Jaques and Fitzgerald 1982) and North Haig (Prinz et al. 1986) also contain fassaitic pyroxenes, but these contain no more than 8 wt% Al_2O_3 and 2 wt% TiO_2. The two Ti-rich pyroxenes in EET 96001,7 are, by comparison, extremely fassaitic (Table 1). Moreover, the DaG 319, Nilpena and North Haig fassaitic pyroxenes occur in angrite-like clasts with $An_{98–99}$ plagioclase, and in the case of the DaG 319 clast, angrite-like O isotopes (Kita et al. 2004), whereas none of the feldspar found in EET 96001 is more anorthitic than An_{63}. In terms of glasses, of eight feldspathic glasses found in DaG 319 by Ikeda et al. (2000), three have high K_2O/Na_2O comparable to the EET 96001 glasses, but five have much lower K_2O/Na_2O (0–0.15; for comparison the lowest value

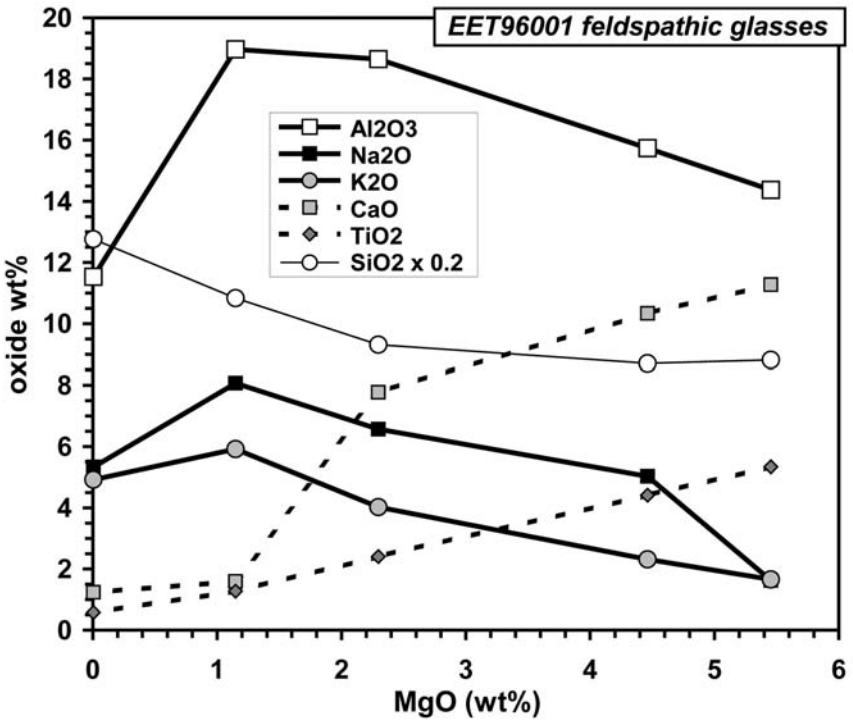

Fig. 10. Compositions of feldspathic glasses in EET 96001. The one major oxide not shown (FeO) is relatively constant among the five glasses analyzed; cf. Table 1.

for EET 96001 glass is 0.46). The average EET 96001 glass (Table 1) has 2.5× higher K and 3.3× higher Ti than the average DaG 319 glass. However, some DaG 319 glasses are associated with ilmenite (Cohen et al. 2004).

In any event, as already discussed, the subvolume of EET 96001 sampled as EET 96001,7 is manifestly, based on texture as well as uniform silicate compositions (apart from the traces of silicates entrained in the distinctive Fe,S-rich veins), a monomict breccia.

Chronology of Brecciation, Cooling, and Ingress of Feldspathic Matter

As noted above, some brecciation prior to introduction of the Fe,S-rich feldspathic veins is suggested by the presence of Fe,S-rich veins within some large, brecciated but optically continuous mafic silicate grains, but the brecciation was not particularly intense. The shock stage is moderate (s2).

Neither the low-Ti ferroan nor the fassaitic pyroxenes, nor the silicas, nor even the most magnesian of the melts (glasses), equilibrated with the host ureilite. Also, the veins appear to have crystallized not homogeneously but starting against their walls. It thus seems likely that at the time the Fe,S-rich veins were emplaced the host rock had cooled somewhat from its condition during the prior anatexis by which its original chondritic complement of feldspathic matter had been removed. Anatexis probably occurred close to 1240 °C, by analogy with moderate-mg ureilites studied by Singletary and Grove (2003). On the other hand, the highly irregular, even convoluted texture of the walls along the "north" end of vein 1B (Fig. 6) suggest that the host ureilite was still warm enough to be susceptible to localized melting in reaction to the introduction of the hot Fe,S vein.

Like most olivines in ureilites, the olivines at the margins of the Fe,S-rich veins typically show strong rim reduction. Evidence of a late, disequilibrium redox process, or "smelting," is a characteristic feature of ureilites. However, this abortive form of smelting should not be confused with the hypothesis (e.g., Singletary and Grove 2003) that at an earlier stage most ureilites underwent more thorough equilibrium smelting that affected the cores of their mafic silicates. The equilibrium smelting hypothesis has been criticized, mainly on the basis of its implication of an implausibly high yield of CO gas, by Warren and Huber (2006).

Conceivably, the abortive smelting of EET 96001 took place entirely prior to the introduction of the present veins. But the largest vein (1A) is highly porous. Depending upon where its terminations are assumed to lie, its overall porosity is roughly 30 vol%. Large-scale porosity is extremely rare among ureilites, and it is possible that all of the apparent porosity in vein 1A is merely an artifact of plucking during thin section preparation. However, the Fe,S oxides that make up most of the solid component of the veins typically contain angular-linear systems of cracks (Fig. 5). Plucking during sample preparation might therefore be expected to leave angular-linear boundaries between the void spaces and the

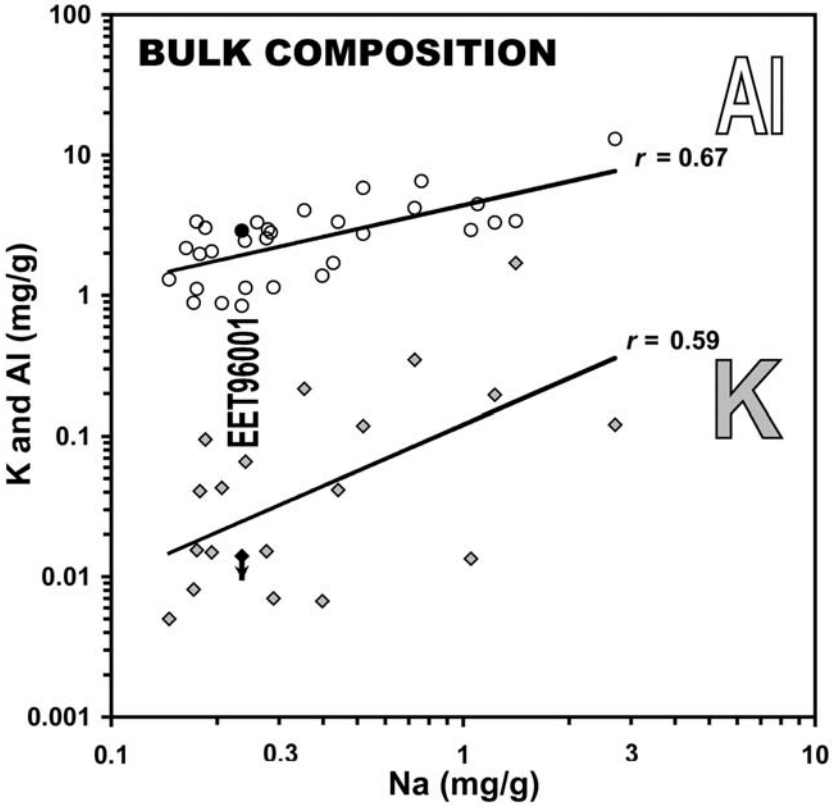

Fig. 11. The bulk composition of EET 96001: lithophile, feldspar-associated elements, with literature data (review Warren et al. 2006) shown for comparison. EET 96001 is not particularly rich in any of the three elements shown.

remnant Fe,S oxide vein groundmass. Instead, the observed boundaries show a marked tendency to appear undulate, or mammilary (Fig. 5). Another curious feature of the void distribution within vein 1A is a tendency to everywhere leave a thick selvage of Fe,S oxide attached to the adjacent mafic silicates. Possibly these aspects of the void distribution merely reflect a tendency for plucking to be controlled by the underlying undulate-banded structure of the Fe,S oxides instead of by the angular-linear cracks. However, structural relationships involving banding, cracks, and obvious weathering products within cracks, suggest that most of the void space in vein 1A is natural, not artificial. Conceivably the porosity originated when some of the Fe,S oxide was removed by the natural process of weathering. However, systematic weathering-removal of Fe,S oxide would probably have yielded a bulk composition uncommonly depleted in siderophile elements; however, just the opposite is observed (Fig. 12).

Assuming the vein porosity is preterrestrial, it suggests that the "smelting" of the olivine rims, a reaction that yields copious proportions of CO gas, took place, at least in part, after the emplacement of the Fe,S-rich veins. The "smelting" reaction is basically reduction of FeO to Fe accompanied by oxidation of C to CO (gas). A slightly more detailed expression (Warren and Huber 2006) is:

$$C + MgFeSiO_4 = MgSiO_3 + Fe + CO \quad (1)$$

The reaction may have sometimes been more like:

$$2C + 2(MgFeSiO_4) = Mg_2SiO_4 + 2Fe + 2CO + SiO_2 \quad (2)$$

but either way, the process engenders a huge volume proportion of CO gas. The grossly incomplete extent of the olivine smelting process attests to a sudden transition to rapid cooling soon after the commencement of the ureilite smelting.

Provenance, Admixture, and Emplacement of Feldspathic Matter

The derivation of the EET 96001 feldspathic component is frankly enigmatic. Much of this section will perforce be speculative. We assume the feldspathic matter was mostly derived from a single, spatially limited source zone (note that this is not meant to connote a source "region" in the anatectic-petrologic sense). Apart from Occam's razor, this assumption seems justified by the preponderance, albeit not the exclusive existence, of a single distinctive compositional trend among the feldspars (Fig. 9).

Several observations suggest that the source zone was a rapidly cooling, near-surface setting, not a pluton. The prevalence of quenched feldspathic glass implies rapid

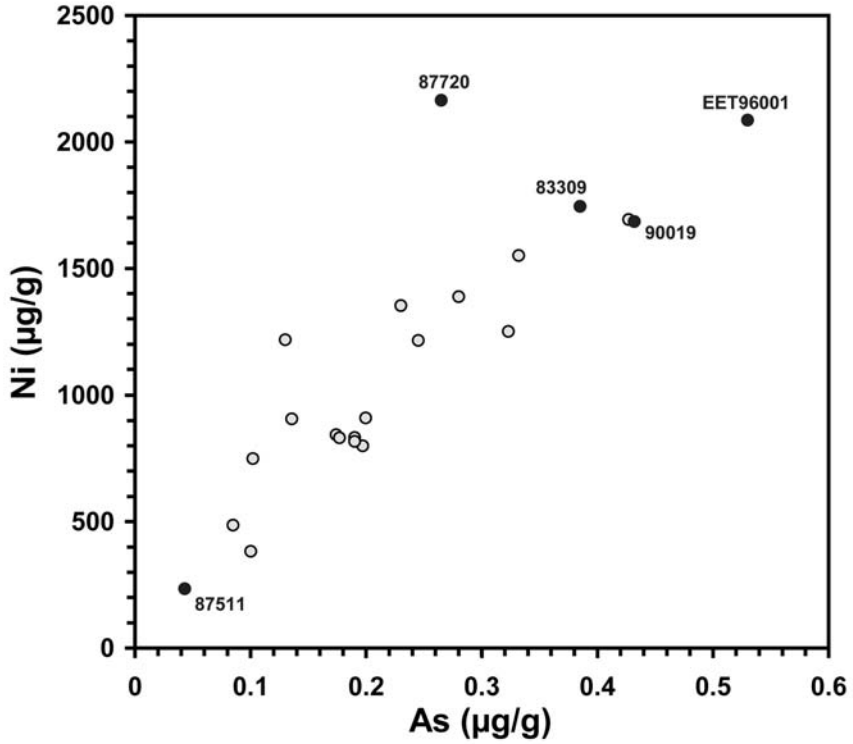

Fig. 12. The bulk composition of EET 96001: moderately siderophile elements Ni and As with literature data, mostly from Warren et al. (2006), shown for comparison. EET 96001 is uncommonly rich in both As, Ni, and siderophile elements in general. Similarity between EET 96001 and EET 83309 (and EET 87220) is discussed in text. Apparent similarity to EET 90019 must be insignificant, because EET 90019 is vastly more magnesian (olivine-core mg ~89 mol%).

cooling. The high proportion of feldspar in the mode for the exotic-seeming vein materials, 32% if glasses are excluded (and conceivably higher still, considering that some of the vein silica might be "smelted" rim material from the host ureilite), suggests a crustal provenance. More speculatively, the large Fe^{3+} component of the spinel included in fassaite 1W seems to require an episode in which the low-fO_2 type of basaltic melt expected from ureilite anatexis was exposed to and assimilated a highly oxidizing component. One conceivable setting for this development would be at or just below the cool surface of the asteroid, where primitive, and water-bearing, carbonaceous chondritic matter had until then survived, even though the deep interior of the asteroid was undergoing anatexis. Of course, a shallow, feldspar-enriched zone implies that the parent asteroid had at least a thin basaltic crust. However, the dearth of feldspar among ureilites in general, and especially among polymict ureilites, still implies a major loss of basaltic component from the parent asteroid(s) (cf. Warren et al. 2006).

Although the glassy components imply shallow provenance for the feldspathic matter, the Fe,S-rich vein groundmass matter must have been extraordinarily dense when emplaced as S-rich metallic melt. Once melted, such material would not be expected to aggregate anywhere near the surface of an asteroid. Although Keil and Wilson (1993) proposed that dense metallic melts might, if buoyed by sufficient proportions of associated gas, ascend toward an asteroidal surface, this model's essential premise is that gas bubbles get explosively larger and larger as the metallic melt-magma nears the surface. This process inevitably results in the metallic melt-magma undergoing explosive dispersal, to the point of permanent removal off the asteroid, once it approaches the vacuous surface. The ultimate provenance of the Fe,S-rich vein groundmass matter was presumably at least a short distance below the top of the anatectic region of the primary asteroid's mantle.

We can only speculate as to how shallow-formed felsic glasses came to be mingled into hot, dense, descent-prone S-rich metallic melts, and then together these oozed through a lightly brecciated ureilite, probably at just about the same time, or soon after, it began to undergo the olivine-FeO "smelting" and rapid cooling that are general characteristics of ureilites. However, such a sequence of developments is conceivable as a rare occurrence, albeit not expected as a typical outcome, in the context of models previously proposed for the late stages of ureilite petrogenesis.

The mechanism that engendered the ureilites' distinctive, extremely step-wise cooling history (Miyamoto et al. 1985) is inferred to have been late-stage disruption of the ureilite-parent asteroid(s); and the disruption is plausibly assumed to

have been triggered by a major impact (Takeda et al. 1989; Warren and Kallemeyn 1992; Scott et al. 1993; Goodrich et al. 2004). As discussed by Warren and Huber (2006), a major impact into a ureilitic asteroid, if it occurred during the formative anatectic stage, might have only served as initial impetus for a more complicated process that ultimately caused a comprehensive disruption of the asteroid. Once the parent asteroid(s), primed with ~3 wt% of mantle carbon, became so hot that several percent (say 5–10%) of melt was stewing in much of its mantle, it was ripe for an episode of "runaway smelting." If, in this delicate state, a major portion (say, one-quarter) of the partly molten body was spalled away, then enormous impetus was given to "smelting" because, like any process that engenders a major proportion of gas (CO) starting from condensed phases, the smelting process is extremely pressure-sensitive (Warren and Huber 2006). Apart from the immediate diminution of interior pressures associated with the putative blast-off of one-quarter of the asteroid's mass, there would soon be further diminution due to loss of melt from the environment of the impact (and, probably, its antipode), as conduits suddenly opened for melt to reach the surface, where the Wilson and Keil (1991) explosive basalt-loss mechanism probably operated. As these authors noted (cf. Warren and Kallemeyn 1992; Scott et al. 1993), eruption of basalt on a low-gravity, atmosphereless body leads to explosive expansion of any gas bubbles. For moderately volatile-rich magmas erupting into near-zero atmospheric pressure—and ureilites formed in an environment with abundant potential CO—the explosive force could suffice to propel nearly all of the silicate melt clear away from the feeble gravitational bond of the asteroid.

The heavily impacted ureilite-parent asteroid would thus enter into a runaway smelting mode: pressure loss causing mass loss causing pressure loss and so on, which would continue through a stage of temporary gross inflation into a very loosely bound rubble pile until the remaining materials, fast-cooling because scattered and suddenly purged of whatever ^{26}Al had remained in the melt, became so cool and melt-purged that the endothermic reaction (1) could not continue. As discussed by Warren and Kallemeyn (1992), the steep thermal gradients implied for the mantle rubble remnants would have presented an almost ideal scenario for the "thermal migration" mechanism advocated by Walker and Agee (1988) for purging of melt from the ureilites; and the CO-rich nature of the ensuing eruptions would have triggered the Wilson and Keil (1991) basalt-loss effect. Remarkably efficient purging of melt has been inferred based on the dearth of feldspar (i.e., basaltic matter), especially among monomict ureilites (Warren and Kallemeyn 1992; Scott et al. 1993).

As soon as their declining temperatures put a break on runaway smelting, the scattered solid materials would mostly reaccrete, or recompact, into a few, possibly just one, altered, partially-reduced and thoroughly melt-purged smaller versions of the original parent asteroid. The principal nucleus for the reaccretion would probably be the primary asteroid's S-rich metallic core (inferred from siderophile element systematics) (Warren et al. 2006), which although mostly molten at the time of the impact would be more cohesive (more ductile, less prone to react to the post-impact pressure drop as a runaway gas-maker, and also well shielded from the impact per se) in comparison to the silicate portion. The reaccretion process must have been selective in that basaltic melt droplets exploded out by the Wilson-Keil process generally traveled too far off to be recaptured.

An interesting corollary of this hypothesis is that the blow-apart process presumably caused considerable jumbling of the pre-impact materials. In a general, statistical way, materials of shallow provenance probably remained shallow in the final, reassembled asteroid, materials of deep provenance probably remained deep, and so forth. However, in a small minority of locales there would inevitably also be incongruous juxtapositions of shallow-provenance with deep-provenance materials. Such may have been the case with EET 96001. We speculate that blow-apart/reassembly jumbling caused cool, shallow-provenance feldspathic component(s) to become mixed into a mass of hot, deep-provenance Fe,S-rich vein matter, which, while still hot enough to flow, became embedded within a mass of lightly brecciated moderate-mg ureilite. This host ureilite was highly permeable because it was still inflated by gas produced in the "smelting" process that engendered the reduced mafic-silicate rims. This is a reasonable supposition because, as a premise of the overall model, the impact-disruption that causes the mixing of the three originally distant materials is caused mainly by "runaway" smelting. Thus, perhaps driven in part by outflow of gases from the last gasps of "smelting," the Fe,S-rich vein matter percolated a short distance through the volume of the host ureilite. However, the percolation did not come close to achieving a clean separation of the dense Fe,S-rich matter from the silicates, and glasses survived within the entrained feldspathic materials, because the material (as with all ureilites: Miyamoto et al. 1985) underwent rapid cooling in its new condition as a parcel randomly located within a smaller, ^{26}Al-depleted daughter-body of the original ureilitic asteroid.

This is admittedly a speculative explanation for emplacement of the EET 96001 feldspathic component. However, such an unusual juxtaposition of materials almost demands that an atypical series of events occurred. The scenario we have proposed seems a logical extension, as a suitably rare occurrence, of a model basically formulated many years ago to account for more general features of ureilite petrology (Warren and Kallemeyn 1992; Scott et al. 1993).

Origin of the Feldspathic Component

EET 96001 is merely one small monomict ureilite. Far more data are available for feldspathic components from polymict ureilites (Ikeda et al. 2000; Cohen et al. 2004; Kita et al. 2004). However, as discussed by Warren et al. (2006),

there is little reason to be confident that the polymict ureilites' tiny component of feldspathic matter is representative of the overall melt products from the parent asteroid(s). According to the explosive volcanism basalt-loss scenario (Warren and Kallemeyn 1992; Scott et al. 1993), the blown-off basalt mostly never reaccreted to the parent asteroid. Survival against the efficient basalt blow-off process might have favored material that was atypical, e.g., erupted late compared to most of the basalt. Late-erupted basalts may have been atypical for various reasons. For example, as suggested by Kita et al. (2004), they might have come from regions depleted by prior cycles of more "normal" melting. The derivation of the EET 96001 feldspathic component is, at best, similarly obscure, but it might be just as representative as the more widely studied feldspathic components in polymict ureilites.

As already discussed, the EET 96001 feldspathic component appears to have come mainly from a shallow basaltic zone. We assume that this basaltic region was a thin crust on a primary ureilite parent body. Provenance from a separate nonureilitic body seems especially unlikely in the case of EET 96001, where the feldspathic component is confined within the Fe,S-rich veins, as opposed to the polymict ureilites, where the feldspars occur in lithic and mineral clasts randomly scattered within a polymict impact breccia. Although the parent magma(s) was shallow and rapid-cooling, the abundance of silica and the wide range of feldspar compositions suggest that it underwent at least limited, interstitial fractional crystallization while near the surface of the asteroid.

Most of the feldspars of EET 96001 have distinctively high K/Na ratio in comparison to the feldspars found in polymict ureilites (Fig. 9). Although the feldspars (Fig. 9) feature a wide range of K/Na, ranging (if a few outliers are ignored) over a factor of 8, note that for the feldspathic glasses, including two that contain analyzed $An_{3–64}$ plagioclases and range in MgO from 5.5 down to 0.01 wt%, K/Na ranges only over a factor of 2.2 (Table 1, Fig. 10). The glass in clast B1 of the polymict ureilite DaG 319 (Cohen et al. 2004) is more EET 96001–like (3.2–3.6 wt% Na_2O, 3.2–3.8 wt% K_2O) than the plagioclase ($An_{5.7}$, 0.6 wt% K_2O) of the same clast. The displacement between the EET 96001 plagioclase trend and the central tendency of the polymict trend on Fig. 9 is clearly a factor of ~8 at the An = 0 intercept. At higher An (say An >20), the data are sparser and the magnitude of the displacement is less clearly defined (are the highest-An compositions in each population fully related to the rest of the material?), but it appears to be at least a factor of 4, and least-squares fitting, excluding the two aberrantly low-K/Na points from EET 96001, suggests it remains ~8.

Kita et al. (2004) employed diagrams similar to Fig. 9 to interpret and model the feldspathic components of polymict ureilites. They compared the ureilite data with results from models that they produced for the origin of feldspathic components as products of crystallization of partial melts derived from carbonaceous-chondritic starting materials. Kita et al. (2004) modeled melting and crystallization using the MELTS program (Ghiorso and Sack 1995), and noted contrasting results for models assuming fractional fusion versus models assuming equilibrium ("batch") melting. According to these models, the fractional fusion and equilibrium fusion scenarios yield practically identical K/Na results for low-An materials (meaning An less than ~35 mol% for models assuming a CI starting material, or ~45 mol% assuming a CM starting material). However, at high stages of melting the fractional fusion model yields lower K/Na than the batch melting model. Kita et al. (2004) favored batch melting for origin of the magmas parental to the "undepleted" (low-An) feldspars that are predominant in polymict ureilites. However, these authors also inferred from the prevalence of low K/Na (i.e., low K at a given plagioclase An; they also considered data for Ba and other trace elements) among the high-An polymict ureilite feldspars, that melting to produce their "depleted" parent magmas occurred in a fractional style; i.e., by removal of melt in many small increments, rather than in a small number of batches. Cohen et al. (2004) argued based on the prevalence of low-An plagioclase in polymict ureilites that fractional melting was the dominant style of partial melting on the ureilite parent body. However, in contrast with Kita et al. (2004) (and common usage), these authors regarded as "fractional" any model with less than "25%–30% melts" involved.

The approach of Kita et al. (2004) can be applied to the distribution of the An-rich feldspars in EET 96001. To the degree that EET 96001's feldspars, as much as the feldspars in polymict ureilites, are representative of the parent asteroid, we may infer that batch melting was even more prevalent, and fractional melting less common, than inferred by Kita et al. (2004). In fact, the main EET 96001 trend is at too high K/Na, at least at its high-An end, to be fit even by the batch melting model. However, the one previous mention of feldspar in a possibly monomict ureilite, FRO 90168 (Bland 1993), has an especially K-poor composition (Fig. 9).

In assessing whether the overall database for ureilite feldspars (Fig. 9) tends to favor fractional or batch melting, it should be emphasized that even in the polymict ureilites, the vast majority of the feldspars have An far below the threshold (~40 mol%) at which the fractional and batch melting models begin to diverge. Virtually the only compositions that feature higher An are from a single polymict ureilite, DaG 319 (Fig. 9). The only two others at An >35, from EET 83309 (Prinz et al. 1987) and EET 87720 (this work), feature K/Na only barely lower than the EET 96001 trend, and well to the "batch" side of the Kita et al. (2004) models.

For the less anorthitic compositions that predominate among both EET 96001 and polymict feldspars, the igneous fractionation models of Kita et al. (2004) imply that fractional versus batch melting is irrelevant; i.e., variations in K/Na may reflect diversity (heterogeneity) among the starting materials. However, Kita et al. (2004) also noted that local fractional

crystallization probably contributed to the compositional diversity among ureilitic feldspars. Among mean compositions for the various chondrite types, K/Na shows only very limited (factors of a few tens of percent) diversity (e.g., Wasson and Kallemeyn 1988; Jarosewich 1990; however, a few individual CM chondrites feature large K/Na fractionations, including up to 2.2× the group mean in the case of Murray: Kallemeyn and Wasson 1981). Source K/Na heterogeneities might conceivably have arisen through fluid metasomatism during the early stages of heat-up within the parent asteroid(s). Goodrich et al. (2002) invoked "pre-igneous, parent-body aqueous alteration and dehydration" to account for putative Ca/Al fractionations among ureilite starting materials. For recent discussions of evidence for aqueous-evaporative processing on warm primitive asteroids, including formation of halite and sylvite, see Busfield et al. (2004) and Takeda et al. (2003). In any case, low K_2O in low-An feldspar is not a peculiar idiosyncrasy of polymict ureilites. Among the very few extraterrestrial, igneous and low-An feldspars, albite found in "granitoidal" clasts of the Adzhi-Bogdo LL3-6 chondrite plots near the center of the low-An end of the polymict ureilite trend (Fig. 9) at An_3 and 0.58 wt% K_2O (Bischoff et al. 1993); and feldspar from a troctolitic clast in the Barwell L6 chondrite plots only slightly above the polymict ureilite trend at An_{20} and 0.53 wt% K_2O (Hutchison et al. 1988).

Goodrich et al. (2004) noted that fractional melting is expected to be the dominant style of partial melting in a setting where melt extraction is aided by copious amounts of CO gas being generated by smelting. However, Warren and Huber (2006) argue that the only significant "smelting" that affected ureilites did not commence until the parent body or bodies underwent catastrophic disruption with accompanying sharp drops in prevailing lithostatic pressures, i.e., after the ureilites had commenced rapid cooling—and thus ceased significant melting.

CONCLUSIONS

The feldspars of the EET 96001 ureilite occur within Fe,S-rich veins that appear to have entered this monomict breccia by a gentle, percolative process, not by violent impact-injection. The feldspars are accompanied by a remarkably diverse suite of K-rich, and frequently Ti-rich, feldspathic glasses, and also major proportions of silica and pyroxene, which is largely fassaitic. This feldspathic component was probably once part of a thin basaltic crust on a ureilite asteroid. A high fO_2 is implied by the apparent oxidation state of iron (~41 atom% Fe^{3+}) in spinel included in one of the fassaites, suggesting that the parent magma may have assimilated near-surface water (however, this fassaite is conceivably unrelated to the typical feldspar). We speculate that the feldspathic component was mixed into the dense, Fe,S-rich vein material, and very soon thereafter the Fe,S-rich vein material was emplaced adjacent to the EET 96001 host ureilite, at an advanced stage in a chaotic catastrophic disruption and partial reassembly process that affected all ureilites.

The K-rich nature of the most of the feldspar and feldspathic glass in EET 96001 suggests that fractional fusion was not as common during ureilite anatexis as has been inferred from recent studies of clasts in polymict ureilites. The newfound diversity for the overall population of ureilite feldspars is probably at least partially reflective of compositional diversity among the starting, pre-anatexis materials. The diversity thus tends to support previous suggestions (Warren and Kallemeyn 1992; Scott et al. 1993) that ureilites might have originated from multiple parent asteroids.

Acknowledgments–We thank J. Berkley and N. Kita for helpful, constructive reviews; also Alan Rubin for helpful advice, and the Meteorite Working Group for allocations of samples. This work was supported by NASA grant NAG5-12819.

Editorial Handling—Dr. Randy Korotev

REFERENCES

Beckett J. R., Grossman L., and Haggerty S. E. 1986. Origin of Ti^{3+}-bearing rhönite in Ca,-Al-rich inclusions: An experimental study (abstract). *Meteoritics* 21:332–333.

Bischoff A., Geiger T., Palme H., Spettel B., Schultz L., Scherer P., Schlüter J., and Lkhamsuren J. 1993. Mineralogy, chemistry, and noble gas contents of Adzhi-Bogdo—An LL3-6 chondritic breccia with L-chondritic and granitoidal clasts. *Meteoritics* 28: 570–578.

Bland P. A. 1993. FRO 90168. *EuroMet Bulletin* 21:5.

Buchanan P. C., Noguchi T., Bogard D. D., Ebihara M., and Katayama I. 2005. Glass veins in the unequilibrated eucrite Yamato-82202. *Geochimica et Cosmochimica Acta* 69:1883–1898.

Busfield A., Gilmour J. D., Whitby J. A., and Turner G. 2004. Iodine-xenon analysis of ordinary chondrite halide: Implications for early solar system water. *Geochimica et Cosmochimica Acta* 68: 195–202.

Cohen B. A., Goodrich C. A., and Keil K. 2004. Feldspathic clast populations in polymict ureilites: Stalking the missing basalts from the ureilite parent body. *Geochimica et Cosmochimica Acta* 68:4249–4266.

Ghiorso M. S. and Sack R. O. 1995. Chemical mass transfer in magmatic processes. *Contributions to Mineralogy and Petrology* 119:197–212.

Goodrich C. A., Krot A. N., Scott E. R. D., Taylor G. J., Fioretti A. M., and Keil K. 2002. Formation and evolution of the ureilite parent body and its offspring (abstract #1379). 33rd Lunar and Planetary Science Conference. CD-ROM.

Goodrich C. A., Scott E. R. D., and Fioretti A. M. 2004. Ureilitic breccias: Clues to the petrologic structure and impact disruption of the ureilite parent asteroid. *Chemie der Erde* 64:283–327.

Greshake A. and Stöffler D. 2000. Shock-related melting phenomena in the SNC meteorite Dar al Gani 476 (abstract #1043). 31st Lunar and Planetary Science Conference. CD-ROM.

Guan Y. and Crozaz G. 2001. Microdistributions and petrogenetic implications of rare earth elements in polymict ureilites. *Meteoritics & Planetary Science* 36:1039–1056.

Hutchison R., Williams C. T., Din V. K., Clayton R. N., Kirschbaum C., Paul R. L., and Lipschutz M. E. 1988. A planetary, H-group pebble in the Barwell, L6, unshocked chondritic meteorite. *Earth and Planetary Science Letters* 90: 105–118.

Ikeda Y., Prinz M., and Nehru C. E. 2000. Lithic and mineral clasts in the Dar al Gani (DAG) 319 polymict ureilite. *Antarctic Meteorite Research* 13:177–221.

Jaques A. L. and Fitzgerald M. J. 1982. The Nilpena ureilite, an unusual polymict breccia: Implications for origin. *Geochimica et Cosmochimica Acta* 46:893–900.

Jarosewich E. 1990. Chemical analyses of meteorites: A compilation of stony and iron meteorite analyses. *Meteoritics* 25:323–337.

Kallemeyn G. W. and Wasson J. T. 1981. The compositional classification of chondrites—I. The carbonaceous chondrite groups. *Geochimica et Cosmochimica Acta* 45:1217–1230.

Keil K. and Wilson L. 1993. Explosive volcanism and the compositions of cores of differentiated asteroids. *Earth and Planetary Science Letters* 117:111–124.

Kita N. T., Ikeda Y., Togashi S., Liu Y., Morishita Y., and Weisberg M. K. 2004. Origin of ureilites inferred from a SIMS oxygen isotopic and trace element study of clasts in the Dar al Gani 319 polymict ureilite. *Geochimica et Cosmochimica Acta* 68:4213–4235.

Mason B. 1998. EET 96001 thin section (,3) description. *Antarctic Meteorite Newsletter* 21:7.

Mittlefehldt D. W., McCoy T. J., Goodrich C. A., and Kracher A. 1998. Non-chondritic meteorites from asteroidal bodies. In *Planetary materials,* edited by Papike J. J. Washington, D.C.: Mineralogical Society of America. pp. 4-1–4-195.

Miyamoto M., Takeda H., and Toyoda H. 1985. Cooling history of some Antarctic ureilites. Proceedings, 16th Lunar and Planetary Science Conference. pp. D116–D122.

Nazarov M. A., Patchen A., and Taylor L. A. 2000. Rhönite-bearing Ca,Al-rich inclusions of the Efremovka (CV3) chondrite (abstract #1242). 31st Lunar and Planetary Science Conference. CD-ROM.

Ott U., Löhr H. P., and Begemann F. 1993. Solar noble gases in polymict ureilites and an update on ureilite noble gas data (abstract). *Meteoritics* 28:415–416.

Prinz M., Weisberg M. K., Nehru C. E., and Delaney J. S. 1986. North Haig and Nilpena: Paired polymict ureilites with Angra dos Reis-related and other clasts (abstract). 17th Lunar and Planetary Science Conference. pp. 681–682.

Prinz M., Weisberg M. K., Nehru C. E., and Delaney J. S. 1987. EET 83309, a polymict ureilite: Recognition of a new group (abstract). 18th Lunar and Planetary Science Conference. pp. 802–803.

Rai V. K., Murthy A. V. S., and Ott U. 2003. Nobles gases in ureilites: Cosmogenic, radiogenic, and trapped components. *Geochimica et Cosmochimica Acta* 67:4435–4456.

Roedder E. and Weiblen P. W. 1977. Shock glass veins in some lunar and meteoritic samples—Their nature and possible origin. Proceedings, 8th Lunar Science Conference. pp. 2593–2615.

Rubin A. E. 2006. Shock, post-shock annealing and post-annealing shock in ureilites. *Meteoritics & Planetary Science* 41:125–133.

Rubin A. E., Keil K., Taylor G. J., Ma M.-S., Schmitt R. A., and Bogard D. D. 1981. Derivation of a heterogeneous lithic fragment in the Bovedy L-group chondrite from impact-melted porphyritic chondrules. *Geochimica et Cosmochimica Acta* 45: 2213–2228.

Scott E. R. D., Taylor J. G., and Keil K. 1993. Origin of ureilite meteorites and implications for planetary accretion. *Geophysical Research Letters* 20:415–418.

Singletary S. J. and Grove T. L. 2003. Early petrogenetic processes on the ureilite parent body. *Meteoritics & Planetary Science* 38: 95–108.

Stöffler D., Keil K., and Scott E. R. D. 1991. Shock metamorphism of ordinary chondrites. *Geochimica et Cosmochimica Acta* 55: 3845–3867.

Takeda H., Mori H., and Ogata H. 1989. Mineralogy of augite-bearing ureilites and the origin of their chemical trends. *Meteoritics* 24:73–81.

Takeda H., Hsu H., and Huss G. R. 2003. Mineralogy of silicate inclusions of the Colomera IIE iron and crystallization of Cr-diopside and alkali feldspar from a partial melt. *Geochimica et Cosmochimica Acta* 67:2269–2287.

Walker D. and Agee C. B. 1988. Ureilite compaction. *Meteoritics* 23: 81–91.

Warren P. H. and Kallemeyn G. W. 1992. Explosive volcanism and the graphite-oxygen fugacity buffer on the parent asteroid(s) of the ureilite meteorites. *Icarus* 100:110–126.

Warren P. H. and Kallemeyn G. W. 1995. QUE 93069: A lunar meteorite rich in HASP glasses (abstract). 26th Lunar and Planetary Science Conference. pp. 1665–1666.

Warren P. H. and Huber H. 2006. Ureilite "smelting" and the catastrophic disruption hypothesis. *Meteoritics & Planetary Science* 41(6).

Warren P. H., Ulff-Møller F., Huber H., and Kallemeyn G. W. 2006. Siderophile geochemistry of ureilites: A record of early stages of planetesimal core formation. *Geochimica et Cosmochimica Acta* 70: 2104–2126.

Wasson J. T. and Kallemeyn G. W. 1988. Compositions of chondrites. *Philosophical Transactions of the Royal Society of London A* 325:535–544.

Wilson L. and Keil K. 1991. Consequences of explosive eruptions on small solar system bodies: The case of the missing basalts on the aubrite parent body. *Earth and Planetary Science Letters* 104: 505–512.